

1 Autumn – winter minimum temperature changes in the 2 southern Sikhote-Alin mountain range of northeast Asia since 3 1529 AD

4 Olga N. Ukhvatkina, Alexander M. Omelko, Alexander A. Zhmerenetsky, Tatyana Y. Petrenko.

5
6 Federal Scientific center of the East Asia terrestrial biodiversity Far Eastern Branch of Russian
7 Academy of Sciences, Vladivostok 690022 RUSSIA

8
9 *Correspondence to:* Olga Ukhvatkina (ukhvatkina@gmail.com)
10

11 **Abstract.** The aim of our research was to reconstruct climatic parameters (for the first time for the Sikhote-Alin
12 mountain range) and to compare them with global climate fluctuations. As a result, we have found that one of the
13 most important limiting factors for the study area is the minimum temperatures of the previous autumn-winter
14 season (August-December), and this finding perfectly conforms to that in other territories. We reconstructed the
15 previous August-December minimum temperature for 485 years, from 1529 to 2014. We found twelve cold periods
16 (1538-1543, 1549-1554, 1643-1649, 1659-1667, 1675-1689, 1722-1735, 1791-1803, 1807-1818, 1822-1827, 1836-
17 1852, 1868-1887, 1911-1925) and seven warm periods (1561-1584, 1603-1607, 1614-1618, 1738-1743, 1756-1759,
18 1776-1781, 1944-2014). These periods correlate well with reconstructed data for the Northern Hemisphere and the
19 neighboring territories of China and Japan. Our reconstruction has 3, 9, 20 and 200-year periods, which are may be
20 in line with high-frequency fluctuations in ENSO, the short-term solar cycle, PDO fluctuations and the 200-year
21 solar activity cycle, respectively. We suggest that the temperature of North Pacific expressed by Pacific Decadal
22 Oscillation has largest contribution in regional climate variations. We have confirmed the climatic response to solar
23 activity, which corresponds to cold periods during the solar minimum. These comparisons show that our climatic
24 reconstruction based on tree-ring chronology for this area may potentially provide a proxy record for long-term,
25 large-scale past temperature patterns for northeast Asia. The reconstruction reflects the global traits and local
26 variations in the climatic processes of the southern territory of the Russian Far East for more than the past 450 years.

27 1 Introduction

28 Global climate change is the main challenge for human life and natural systems, which is why we should clearly
29 understand climatic changes and their mechanisms. A retrospective review of climatic events is necessary for
30 understanding the climatic conditions from a long-term perspective. At the same time, instrumental climate
31 observations rarely cover more than a 100-year period and are often restricted to 50-70 years. This restriction forces
32 the researchers to continuously find new ways and methods to reconstruct climatic fluctuations. Dendrochronology
33 has been widely applied in climatic reconstruction for local territories and at the global scale for both climatic
34 reconstructions of the past few centuries and paleoclimatic reconstructions because it is rather precise, extensively
35 used and a replicable instrument (Corona et al.; Popa and Bouriaund, 2014; Kress et al., 2014; Lyu et al., 2016).
36 A great number of studies have focused on climatic change reconstruction for the northeastern parts of China based
37 on *P. koraeinsis* radial growth studies (e.g., Zhu et al., 2009; Wang et al., 2013; Wang et al., 2016; Zhu et al., 2015;
38 Lyu et al. 2016). Climatic parameters were reconstructed for the whole Northern Hemisphere (Wilson et al., 2016),
39 China (Ge et al., 2016), and temperature characteristics were reconstructed for northeastern Asia (Ohyama et al.,
40 2013). Despite this, there are very few studies of Russian Far East climate (e.g., Willes et al., 2014; Jacoby et al.,
41 2004; Shan et al., 2015); moreover, there is an absence of dendrochronological studies for the continental part of

42 Russian Far East. Meanwhile, most of species present in northeastern China, the Korean peninsula and Japan grow in
43 this region. In addition, the distribution areas of these trees often end in the south of the Russian Far East, which
44 increases the climatic sensitivity of plants. Additionally, some parts of the forests in the Russian Far Eastern have not
45 been subjected to human activity for the last 2000-4000 years. This makes it possible to forests extend the studied
46 timespan. In addition, the southern territory of the Russian Far East is sensitive to global climatic changes as it is
47 under the influence of cold air flow from northeastern Asia during the winter and summer monsoons. All of the factors
48 listed above create favorable conditions for dendroclimatic studies.

49 It is well-known that cold and warm periods of the climate is correlated with intensive solar activity (e.g., the Medieval
50 Warm Period), while decreases in temperature occurs during periods of low solar activity (e.g., the Little Ice Age;
51 Lean and Rind, 1999; Bond et al., 2001). According to findings from an area of China neighboring the territory studied
52 here, the registered warming has been significantly affected by global warming since the 20th century (Ding and Dai,
53 1994; Wang et al., 2004; Zhao et al., 2009), which is often indicated by a faster rise in night or minimum temperatures
54 (Karl et al., 1993; Ren and Zhai, 1998; Tang et al., 2005). To better understand and evaluate future temperature change
55 trends, we should study the long-term history of climatic changes.

56 However, using tree-ring series for northeastern Asia (particularly temperature) is rather complicated due to the unique
57 hydrothermal conditions of the region. Most reconstructions cover periods of less than 250 years (e.g., Shao and Wu,
58 1997; Zhu et al., 2009; Wang et al., 2012; Li and Wang, 2013; Yin et al., 2009; Zhu et al., 2015), except for a few
59 with periods up to 400 years (Lyu et al., 2016; Wiles et al., 2014). The short period of reconstructions is the reason
60 why such reconstructions cannot capture low-frequency climate variations.

61 The warming of the climate (particularly minimum temperature increase) is registered across the whole territory of
62 northeastern Asia (Lyu et al., 2016). In the Russian Far-East, such warming has been recorded for more than 40 past
63 years (Kozhevnikova, 2009). However, the lack of detailed climatic reconstructions for the last few centuries makes
64 it difficult to capture long-period climatic events for this territory and interpret the temperature conditions for the last
65 500-1000 years.

66 Therefore, the main objectives of this study were (1) to develop the first three-ring-width chronology for the southern
67 part of the Russian Far East; (2) to analyze the regime of temperature variation over the past centuries in the southern
68 part of the Russian Far East; (3) to identify the recent warming amplitude in context of long-term changes and to
69 analyze the periodicity of climatic events and their driving forces. Our new minimum temperature record supplements
70 the existing data for northeast Asia and provides new evidence of past climate variability. There is the potential to
71 better understand future climatic trajectories from these data in northeast Asia.

72

73 **2 Materials and methods**

74 **2.1 Study area**

75 We studied the western macroslope of the southern part of the Sikhote-Alin mountain range (Southeastern Russia) at
76 the Verkhneussuriysky Research Station of the Federal Scientific Center of the East Asia terrestrial biodiversity Far
77 East Branch of the Russian Academy of Sciences (4400 ha; N 44°01'35.3'', E 134°12'59.8'', Fig. 1).

78 The territory is characterized by a monsoon climate with relatively long, cold winters and warm, rainy summers. The
79 average annual air temperature is 0.9 °C; January is the coldest month (−32 °C average temperature), and July is the
80 warmest month (27 °C average temperature). The average annual precipitation is 832 mm (Kozhevnikova, 2009).

81 Southerly and southeasterly winds predominate during the spring and summer, while northerly and northwesterly

82 winds predominate in autumn and winter. The terrain includes mountain slopes with an average angle of $\sim 20^\circ$, and
83 the study area is characterized by brown mountain forest soils (Ivanov, 1964) (Fig. 2).

84 Mixed forests with Korean pine (*Pinus koraeensis* Siebold et Zucc.) are the main vegetation type in the study area,
85 and they form an altitudinal belt up to 800 m above sea level. These trees are gradually replaced by coniferous fir-
86 spruce forests at high altitudes (Kolesnikov, 1956). Korean pine-broadleaved forests are formed by up to 30 tree
87 species, with *Abies nephrolepis* (Trautv.) Maxim, *Betula costata* (Trautv.) Regel., *Picea jezoensis* (Siebold et Zucc.)
88 Carr., *P. koraeensis* and *Tilia amurensis* Rupr. being dominant.

89 Korean pine-broadleaved forests are the main forest vegetation type in the Sikhote-Alin mountain range in the
90 southern part of the Russian Far East. This area is the northeastern limit of the range of Korean pine-broadleaved
91 forests, which are also found in northeastern China (the central part of the range), on the Korean peninsula, and in
92 Japan. The Sikhote-Alin mountain range is one of the few places where significant areas of old-growth Korean pine-
93 broadleaved forest remain. In the absence of volcanic activity, which is a source of strong natural disturbances in the
94 central part of the range (Liu, 1997; Ishikava, 1999; Dai et al., 2011), wind is the primary disturbance factor on this
95 territory. Wind causes a wide range of disturbance events, from individual treefalls to large blowdowns (Dai et al.,
96 2011).

97 Approximately 60% of the Research Station area had been subjected to selective clear-cutting before the station was
98 established in 1972. The remaining 40% of its area has never been clear-cut and is covered by unique old-growth
99 forest.

100 2.2 Tree-ring chronology development

101 Our study is based on data collected in a 10.5-ha permanent plot (Omelko and Ukhvatkina, 2012; Omelko et al., 2016),
102 which was located in the middle portion of a west-facing slope with an angle of 22° at a gradient altitude 750-950 m
103 above sea level. The forest in the plot was a late-successional stand belonging to the middle type of Korean pine-
104 broadleaved forests at the upper bound of the distribution of Korean pine, where it forms mixed stands of Korean
105 pine-spruce and spruce-broadleaved forests (Kolesnikov, 1956).

106 One core per undamaged old-growth mature tree (25 cores from 25 trees) and one sample from dead trees (20 samples)
107 were extracted from *P. koraiensis* trees in the sample plots from the trunks at breast height. In the laboratory, all tree-
108 ring samples were mounted, dried and progressively sanded to a fine polish until individual tracheids within annual
109 rings were visible under an anatomical microscope according to standard dendrochronological procedures (Fritts,
110 1976; Cook and Kairiukstis, 1990). Preliminary calendar years were assigned to each growth ring, and possible errors
111 in measurement due to false or locally absent rings were identified using the Skeleton-plot cross-dating method
112 (Stokes and Smiley, 1968). The cores were measured using the semi-automatic Velmex measuring system (Velmex,
113 Inc., Bloomfield, NY, USA) with a precision of 0.01 mm. Then, the COFECHA program was used to check the
114 accuracy of the cross-dated measurements (Holmes, 1983). To mitigate the potential trend distortion problem in
115 traditionally detrended chronology (Melvin and Briffa, 2008; Anchukaitis et al., 2013), we used a signal-free method
116 (Melvin and Briffa, 2008) to detrend the tree-ring series using the RCSigFree program (<http://www.ldeo.columbia.edu/tree-ring-laboratory/resources/software>).

118 Age-related trends were removed from the raw tree-ring series using an age-dependent spline smoothing method. The
119 ratio method was used to calculate tree-ring indices, and the age-dependent spline was selected to stabilize the variance
120 caused by core numbers. Finally, the stabilized signal-free chronology was used for the subsequent analysis (Fig. 3).
121 The mean correlations between trees (*Rbt*), mean sensitivity (MS) and expressed population signal (EPS) were
122 calculated to evaluate the quality of the chronology (Fritts, 1976). *Rbt* reflects the high-frequency variance, and MS

123 describes the mean percentage change from each measured annual ring value to the next (Fritts, 1976; Cook and
124 Kairiukstis, 1990). EPS indicates the extent to which the sample size is representative of a theoretical population with
125 an infinite number of individuals. A level of 0.85 in the EPS is considered to indicate a chronology of satisfactory
126 quality (Wigley *et al.*, 1984). The statistical characteristics of the chronology are listed in Table 1.
127 The full length of the chronology spans (VUS chronology) from 1451 to 2015. A generally acceptable threshold of
128 the EPS was consistently greater than 0.85 from AD 1602 to 2015 (9 trees; Fig. 3b), which affirmed that this is a
129 reliable period. However, although the EPS value from AD 1529 to 1602 was less than 0.85, it matches a minimum
130 sample depth of 4 trees in this segment (EPS>0.75). It is very important to extend the tree-ring chronology as much
131 as possible because there are only a few long climate reconstructions in this area. Therefore, we retained the part from
132 1529 to 1602 in the reconstruction.

133 2.3 Climate data and statistical methods

134 Monthly precipitation, monthly mean and minimum temperature data were obtained from the Chuguevka
135 meteorological station (44.151462 N, 133.869530 E, about 30 km from Verkhneussuriisky research station) and the
136 meteorological post at the Verkhneussuriisky research station of the Federal Scientific Center of the East Asia
137 terrestrial biodiversity FEB RAS (Meteostation 7 – MP7) as well. The periods of monthly data available from the
138 Chuguevka and Verkhneussuriisky stations are 1936-2004 and 1969-2004, respectively (1971-2003 for minimum
139 temperature data from the Chuguevka).

140 The data of large-scale climate conditions, such as the Northern Hemisphere temperature (NH), North Atlantic
141 Oscillation (AMO), Pacific Decadal Oscillation (PDO) and Nino3 reconstruction (Mann *et al.*, 2009), and also
142 indicators of solar activity, such as reconstructed solar constant (TSI, Lean, 2000) and sun spot number (SSN) were
143 downloaded and analyzed in Royal Netherlands Meteorological Institute climate explorer (<http://climexp.knmi.nl>).
144 To demonstrate that our reconstruction representative and reflect temperature variations, we conducted spatial
145 correlation between our temperature reconstruction and gridded temperature dataset of the Climate Research Unit
146 (CRU TS4.00) for the period 1960-2003, by using the Royal Netherlands Meteorological Institute climate explorer
147 (<http://climexp.knmi.nl>).

148

149 2.4 Statistical analyses

150 A correlation analysis was used to evaluate the relationships between the ring-width index and observed monthly
151 climate records from the previous June to the current September. To identify the climate-growth relationships of
152 Korean pine in the southern Sikhote-Alin mountain range, a Pearson's correlation was performed between climate
153 variables and tree-width index. We used a traditional split-period calibration/verification method to explore the
154 temporal stability and reliability of the reconstruction model (Fritts, 1976; Cook and Kairiukstis, 1990). The Pearson's
155 correlation coefficient (r), R-squared (R^2), the reduction of the error (RE) the coefficient of efficiency (CE), and the
156 product means test (PMT) were used to verify the results. Analyses were carried out in R using the treeclim package
157 (Zang and Biondi, 2015) and STATISTICA software (StatSoft®). Analyses of reconstruction included multi-taper
158 method (MTM) (Mann & Lees, 1996) and Monte Carlo Singular Spectrum Analysis (SSA; Allen and Smith, 1996).
159 Analysis was carried out in SSA-MTM Toolkit for Spectral Analysis software (Ghil *et al.*, 2001; Dettinger *et al.*,
160 1995).

161 3 Results

162 3.1 Climate-radial growth relationship

163 Relationships between the VUS chronology and monthly climate data are shown in Fig. 4. To reveal the correlation
164 between climatic parameters and radial growth change of *P. koraiensis*, we had three data sets: the first-time series
165 had a length of 68 years (1936-2004, Chuguevka), the second had a length of 34 years (1966-2000, MP7), and the
166 third had a length of 33 years (1971-2003, Chuguevka, minimum temperature). To select the appropriate parameters,
167 we analyzed all datasets. As a result, we revealed a reliable but slight positive correlation between *P. koraiensis* growth
168 and precipitation in May and June of the current year and September of the previous year in the territory of Chuguevka
169 village (Fig. 4a). There is also a slight positive correlation with precipitation in September of the previous year and
170 May of the current year at Metheostation 7 (MP7) (Fig. 4b). In addition, we revealed a slight negative correlation with
171 precipitation in February-March of the current year.

172 As for the correlation between temperature and *P. koraiensis* growth, the analysis reveals a weak positive correlation
173 with the average monthly temperature in June of the previous year and in February-April of the current year in the
174 Chuguevka settlement and a slight negative correlation with the average monthly temperature in June-July as well
175 (Fig. 4c). The analysis of the correlation with the average monthly temperature at Metheostation 7 (MP7) shows us a
176 weak positive correlation with temperature in August and December of the preceding year and a negative correlation
177 with temperature in July of the current year (Fig. 4d). In addition, we analyzed the correlation with minimum average
178 monthly temperatures at MP7 and Chuguevka. The revealed correlation with minimum temperature is reliable but
179 weak (Fig. 4e,f).

180 Moreover, based on the weak interaction that was revealed, we analyzed the correlation with climatic parameters for
181 selected ranges of months (Fig. 4h,g). The highest significant correlation appears between growth and the minimum
182 monthly temperature of August-December of the previous year at Chuguevka (Fig. 4h), on which we base our
183 subsequent reconstructions.

184 3.2 Minimum temperature reconstruction

185 Basing on analysis of the correlation between climatic parameters and Korean pine growth, we constructed a linear
186 regression equation to reconstruct the minimum monthly temperature of August-December of the previous year
187 (VUSr). The transfer function was as follows:

$$188 \text{VUSr} = 7.189X_t - 15.161$$

$$189 (N=32, R=0.620, R^2=0.385, R^2_{\text{adj}}=0.364, F=18.76, p < 0.001)$$

190 where VUSr is the August-December minimum temperature at Chuguevka and X is the tree-ring index of the Korean
191 pine RSC chronology in year t . The comparison between the reconstructed and observed mean growing season
192 temperatures during the calibration period is shown in Fig. 5(a). The cross-validation test for the calibration period
193 (1971-1997, $R=0.624$) yielded a positive RE of 0.334, a CE of 0.284, and the cross-validation test for calibration
194 period 1977-2003 ($R=0.542$) a positive RE of 0.654, a CE of 0.644, confirming the predictive ability of the model.
195 Although during the study period, the model shows the observed values very well, the short observation period (1971-
196 2003) does not allow using split-sampling calibration and verification methods in full for evaluating quality and model
197 stability. This limitation is why we used a bootstrapping resampling approach (Efron, 1979; Young, 1994) for stability
198 evaluation and transfer function precision. The idea that this method is based on indicates that the available data
199 already include all the necessary information for describing the empirical probability for all statistics of interest.

200 Bootstrapping can provide the standard errors of statistical estimators even when no theory exists (Lui et al., 2009).
201 The calibration and verification statistics are shown in Table 2. The statistical parameters used in bootstrapping are
202 very similar to those from the original regression model, and this proves that the model is quite stable and reliable and
203 that it can be used for temperature reconstruction.

205 3.3 Temperature variations from AD 1529 to 2014 and temperature periodicity

206 Variations in the reconstructed average minimum temperature of the previous August-December (VUSr) since AD
207 1529 and its 21-year moving average are shown in Fig. 5b. The 21-year moving average of the reconstructed series
208 was used to obtain low-frequency information and analyze temperature variability in this region. The mean value of
209 the 486-year reconstructed temperature was -7.93°C with a standard deviation of $\pm 1.40^{\circ}\text{C}$. We defined warm and
210 cold periods as when temperature deviated from the mean value plus or minus 0.5 times the standard deviation,
211 respectively (Fig. 5b). If the reconstructed minimum temperatures were above or below the average value by $>0.5\text{ SD}$
212 for three or more years, then we considered this deviation as warm or cold period, respectively. Also, if two warm (or
213 cold) periods were separated by one year, when the temperature sharply decreased (or increased), then such periods
214 merged into one.

215 Hence, warm periods occurred in 1561-1584, 1603-1607, 1614-1618, 1738-1743, 1756-1759, 1776-1781, 1944-2014,
216 and cold periods appeared in 1538-1543, 1549-1554, 1643-1649, 1659-1667, 1675-1689, 1722-1735, 1791-1803,
217 1807-1818, 1822-1827, 1836-1852, 1868-1887, 1911-1925. Among them, the four warmest years were in 1574 ($-$
218 4.35°C), 1606 (-5.35°C), 1615 (-5.71°C), 1741 (-5.36°C), 1757 (-6.16°C), 1779 (-5.21°C), 2008 (-2.72°C), while
219 the three coldest year were in 1543 (-9.84°C), 1551 (-9.88°C), 1647 (-10.77°C), 1662 (-11.10°C), 1685 (-9.45°C),
220 1728 (-10.08°C), 1799 (-10.70°C), 1815 (-10.13°C), 1825 (-9.87°C), 1843 (-10.55°C), 1883 (-10.73°C), 1913 ($-$
221 10.29°C). The longest cold period extended from 1868 to 1887, and the longest warm period extended from 1944 to
222 present day. The coldest year is 1662 (-11.10°C) and the warmest year is 2008 (-2.72°C).

223 The MTM spectral analysis over the full length of our reconstruction revealed significant ($p < 0.05$) cycle peaks at
224 2.3-year (95%), 2.5-year (99%), 2.9-year (99%), 3.0-year (99%), 3.3-year (95%), 3.7-year (95%), 8.9-year (99%)
225 short periods and 20.4-year (95%), 47.6-year (95%), 188.7-year (99%) long periods (Fig. 6). Singular spectrum
226 analysis (SSA) reveals 8 leading temporal modes that significant at the 95% confidence level (Allen & Smith, 1996).
227 Of these, SSA analysis reveals a single significant low order mode variability near 200 years, but there is little evidence
228 in the reconstruction variability at the 40-50 years. Also 3 significant power periods were reveals: 20.4-year, 9-year
229 and near 3-year periods. Comparison of the reconstruction and global temperature for oceans of Northern Hemisphere
230 (NH), North Atlantic Oscillation (AMO), Pacific Decadal Oscillation (PDO) and Nino3 reconstruction (Mann et al.,
231 2009) show significant correlation between reconstruction and NH ($r=0.67$, $p<0.0001$), AMO ($r=0.49$, $p<0.001$), and
232 PDO ($r=0.68$, $p<0.0001$), and non-significant correlation between reconstruction and Nino3 reconstruction ($r=0.27$,
233 $p=0.08$). Comparison of the reconstruction and indicators of solar activity shows significant correlation of the
234 minimum temperature with the TSI ($r=0.52$, $p<0.0001$) and non-significant correlation with SSN ($r=0.26$, $p<0.1$).

235 Spatial correlations between our reconstruction and the CRU TS4.00 temperature dataset reveal our record's
236 geographical representation (Fig. 7). The results show that the reconstruction of mean minimum temperature of
237 previous August – December is significantly positively correlated with the CRU TS4.00 ($r=0.568$, $p<0.0001$).

238 4 Discussion

239 4.1 Climate-growth relationships

240 The results of our analysis suggest that the radial growth of Korean pine in the southern part of the Sikhote-Alin
241 mountain range is mainly limited by the pre-growth autumn-winter season temperatures, in particular the minimum
242 temperatures of August-December (Fig. 4). It is widely known that tree-ring growth in cold and wet ecotopes, situated
243 on sufficiently high elevation in the Northern Hemisphere, strongly correlate with temperature variability in large
244 areas of Asia, Eurasia, North America (Zhu et al., 2009; Anchukaitis et al., 2013; Thapa et al., 2015; Wiles et al.,
245 2014). The limiting influence of temperature on *P. koraiensis* growth has been mentioned in many studies (Wang et
246 al., 2016; Yin et al., 2009; Wang et al., 2013; Zhu et al., 2009). However, the temperature has various limiting effects
247 in different conditions, and these limiting effects manifest in different ways (Wang et al., 2016). For example, Zhu et
248 al., 2016 indicates that in more northern and arid conditions of the Zhangguangcai Mountains, while precipitation is
249 not the main limiting factor, precipitation is considerably below evaporation during the growth season. This finding
250 is why a stable correlation between *P. koraiensis* growth and the growth season temperature is revealed. This finding
251 is also why moisture availability in soil might be the main limiting factor for Korean pine growth (Zhu et al., 2016),
252 but the emergence of this circumstance can be different in different conditions.

253 The correlation between growth and minimum temperatures in August-December of the previous year, as revealed
254 in our research, was also mentioned for Korean pine in other works (Wang et al., 2016; Zhang et al., 2015). This
255 finding may be explained by the following circumstances. Extreme temperatures limit the growth of trees at the tree
256 line or in high-latitude forests (Wilson and Luckman, 2002; Körner and Paulsen, 2004; Porter et al., 2013; Yin et al.,
257 2015). Taking into consideration the fact that the study area is situated at the altitudinal limit of Korean pine forest
258 distributions, in particular the Korean pine (Kolesnikov, 1956), these findings seem to be reliable.

259 In addition, in the conditions close to extreme for this species, low temperatures in autumn-winter may lead to thicker
260 snow cover, which melts far more slowly in spring (Zhang et al., 2015). The study area is notable for its dry spring,
261 and the amount of precipitation is minimal during the most important period of tree-growth in April-May
262 (Kozhevnikova, 2009). If the vegetation period of the plant cannot begin at the end of March and packed snow cover
263 melting is impeded up until the beginning of May, plant growth may be reduced. Moreover, although cambial activity
264 stops in the winter, organic components are still synthesized by photosynthesis. Low temperatures (in the territory of
265 the VUSr it can reach -48°C in certain years) may induce to loss of accumulated materials, which adversely affects
266 growth (Zhang et al., 2015). The study area is in the center of the vegetated area, where the conditions for Korean
267 pine growth are optimal during the growing season, and only minimum temperature is regarded as an extreme factor.

268 4.2 Comparison with other tree-ring-based temperature reconstructions

269 At present, temperature reconstructions are uncommon for the Russian Far East, and research sites are located for
270 thousands of kilometers away from one another. For example, Wiles et al. undertook a study of summer temperatures
271 on Sakhalin Island (Wiles et al., 2014). Unfortunately, it is impossible to compare our findings with theirs because
272 Sakhalin Island is climatically far more similar to Japanese islands than to the Sikhote-Alin mountains, and
273 temperature variations in their study area are mainly caused by oceanic currents.

274 In addition, instrumental observations from the study area rarely encompass a period longer than 50 years (and studies
275 have only been conducted for large settlements). Consequently, the tree-ring record serves as a good indicator of the
276 past cold-warm fluctuations in the Russian Far East. The analysis of spatial correlations between our reconstruction
277 and the CRU TS4.00 temperature dataset reveal spatial correlations between the observed and reconstruction
278 minimum temperatures from the CRU TS4.00 gridded T_{\min} dataset during the baseline period of 1960-2003 (Fig. 7).

279 It's indicating that our temperature reconstruction is representative of large-scale regional temperature variations and
280 can be taken as representative of southeastern of the Russian Far East and northeastern of the China.

281 To identify the regional representativeness of our reconstruction, we compared it with two temperature reconstructions
282 for surroundings areas and a reconstruction for the Northern Hemisphere (Fig. 8). The first reconstruction was for
283 summer temperatures in the Northern Hemisphere (Wilson et al., 2016). The second reconstruction was an April-July
284 tree-ring-based minimum temperature reconstruction for Laobai Mountain (northeast China), which is approximately
285 500 km northwest of our site. The third was a February-April temperature reconstruction for the Changbai Mountain
286 (Zhu et al., 2009), which are approximately 430 km southwest of our site. Although the spring and summer
287 temperatures have been reconstructed in the last two cases, we use these reconstructions for comparison, because,
288 firstly, there are no other reconstructions for this region, and secondly, despite the possible seasonal shifts, long cold
289 and warm periods should be identified in all seasons.

290 Cold and warm periods are shown in table 3 (the duration is given by the authors of the article). The reconstructions
291 show that practically all cold and warm periods coincide but have different durations and intensities. The data on
292 Northern Hemisphere show considerable overlaps of cold and warm periods, and the correlation between
293 reconstructions is 0.45 ($p > 0.001$). At the same time, we found the warm period 1561-1584, which is not clearly
294 shown in reconstruction for the Northern Hemisphere, though the general trend of temperature change is maintained
295 during this period (Fig. 8). Long cold periods from 1643 to 1667 and 1675-1690 that were revealed for another territory
296 (Lyu et al., 2016; Wilson et al., 2016) coincided with the Maunder Minimum (1645–1715), an interval of decreased
297 solar irradiance (Bard et al., 2000). The coldest year in this study (1662) revealed in this period too. The Dalton
298 minimum period centered in 1810 is also notable. Interestingly that cold periods of 1807-1818, 1822-1827, 1836-1852
299 and 1868-1887 is also registered in reconstructions for Asia (Ohayama et al., 2013) and by Japanese researchers
300 (Fukaishi & Tagami, 1992; Hirano & Mikami, 2007). Moreover, instrumental observations reconstructed for western
301 Japanese territories (the nearest to the study area) provide evidence of a cold period in the 1830s-1880s with a short
302 warm spell in the 1850s (Zaiki et al., 2006), which is in agreement with our data (not reliably period 1855-1865, Tabl.
303 3). For this period, there are contemporaneous records of severe hunger in Japan in 1832 and 1839, which was the
304 result of a summer temperature decrease and rice crop failure (Nishimura & Yoshikawa, 1936).

305 In this case, the longer cold period for the study area can be explained by the relatively lower influence of the warm
306 current and monsoon and generally colder climate in the south of the Russian Far East compared with Japanese islands.
307 The differing opinion about the three cold periods in China in the 17th, 18th and 19th centuries (Wang et al., 2003) is
308 also corroborated by our reconstruction. The cold period in the 19th century is even more pronounced than that reported
309 by Lyu et al., 2016. Moreover, Lyu et al., 2016 corroborate that the ascertained cold period in 19th century is more
310 evident in South China, but it is less clear in the northern territories or has inverse trend. Although the Russian Far
311 East is further north than the southern Chinese provinces and is closer to the northern part of the country, the marked
312 monsoon climate likely made it possible to reflect the general cold trend in 19th century, which was typical both for
313 China and the entire Northern Hemisphere. Because of this possible explanation, the cold period in the 19th century
314 for the Changbai Mountains shows up more distinctly than for the northern and western territory of Laobai Mountain
315 (Fig. 8).

316 Apparently, this discrepancy in regional climate flow is the reason that our reconstruction agrees well with the general
317 reconstruction for the whole hemisphere ($r = 0.45, p < 0.001$) and to a lesser extent agrees with the regional curves for
318 Laobai Mountain ($r = 0.23, p < 0.001$) and Changbai Mountain ($r = 0.32, p < 0.001$).

319 The changing dynamics of the 20th century temperature is also interesting to watch. The comparison of the minimum
320 annual temperatures for the territory and the reconstructed data for the period of 1960-2003 shows significant data

321 correlation (Fig. 7), including the northeast part of China. At the same time, for Chinese territory (both for southwest
322 regions and for more northwestern regions), the warming is apparent only in the last quarter century (Zhu et al., 2009)
323 or at the end of the 20th century (Lyu et al., 2016) (Fig. 8 c,d). This trend, revealed for the southern Sikhote-Alin
324 mountains (a warm spell since 1944), is corroborated for the whole Northern Hemisphere (Wilson et al., 2016) (Fig.
325 8a,b). The maximum cold period is also corroborated, which we note for the 19th century (Fig. 8a,b).
326 The probable explanation is in the regional climate flow differences in the compared data. The territory of northeastern
327 China is more continental, though the influence of the Pacific Ocean is also notable. At the same time, the southern
328 part of the Sikhote-Alin mountains is more prone to the influence of monsoons, as are the Japanese islands. According
329 to paleoreconstructions, the Little Ice Age occurred in the Northern Hemisphere 600-150 years ago (Borisova, 2014).
330 The period of landscape formation (vegetation types and altitudinal zonation) for the Sikhote-Alin range during the
331 transition from the Little Ice Age to contemporary conditions occurred within the last 230 years (Razzhigaeva et al.,
332 2016). The timeframe of the Little Ice Age is generally recognized as varying considerably depending on the region
333 (Bazarova et al., 2014). However, it is certain that the Little Ice Age is accompanied by an increase in humidity in
334 coastal areas of northeast Asia (Bazarova et al., 2014). Thus, in similar conditions on the Japanese islands, the Little
335 Ice Age was accompanied by lingering and intensive rains (Sakaguchi, 1983), and the last typhoon activity was
336 registered for the Japanese islands from the middle of the 17th century to the end of the 19th century (Woodruff et al.,
337 2009). At the same time, the reconstruction of climatic changes for the whole territory of China for the last 2000 years
338 (Ge et al., 2016) shows that the cold period lasted until 1920, which correlates with the data we obtained. This timespan
339 wholly coincides with our data, and we can draw the conclusion that in the southern region of the Sikhote-Alin
340 mountains, the Little Ice Age ended at the turn of the 19th century.
341 Unfortunately, when comparing temperature, different changes were also observed for some cold and warm years
342 (Fig. 8). This finding may be attributed to differences in the reconstructed temperature parameters (such as average
343 value, minimum temperature and maximum temperature) and environmental conditions in different sampling regions.
344 Recent studies show that the oscillations in the medium, minimum and maximum temperature are often asymmetrical
345 (Karl et al., 1993; Xie and Cao, 1996; Wilson and Luckman, 2002, 2003; Gou et al., 2008). The global warming over
346 the past few decades has been mainly caused by the rapid growth of night or minimum temperatures but not maximum
347 temperatures. Meanwhile, some differences between the reconstructed temperature values were well explained by a
348 comparison with similar areas.

349 We can conclude that the analysis shows that the reconstructed data is representative for large-scale regional
350 temperature variations (Fig. 7). At the same time, some cold and warm periods in our reconstruction and other
351 neighbored studies do not coincide (Fig. 8), which can be due to the reconstruction of other climatic parameters and
352 differing environmental conditions. So, we believe that these results can characterize regional climate variations and
353 provide reliable data for large-scale reconstructions for the northeastern portion of Eurasia, but their use for large-
354 scale regional reconstructions requires further research.

355 4.3 Periodicity of climatic changes and their links to global climate processes

356 Among the significant periodicities in the reconstructed temperature detected by the MTM analysis (Fig. 7), some
357 peaks were singled out: 2.3-year (95%), 2.5-year (99%), 2.9-year (99%), 3.0-year (99%), 3.3-year (95%), 3.7-year
358 (95%), 8.9-year (99%) short periods and 20.4-year (95%), 47.6-year (95%), and 188.7-year (99%) long periods. SSA
359 analysis shows significant near 3-year, 9-year, 20.4-year and 200-year periods.

360 The 3-year cycle may be linked with the El Niño-Southern Oscillation (ENSO). These high-frequency (2-7-year)
361 cycles (Bradley *et al.*, 1987) have also been found in other tree-ring-based temperature reconstructions in northeast

362 Asia (Zhu *et al.*, 2009; Li and Wang, 2013; Zhu *et al.*, 2016; Gao *et al.*, 2015). The 2–3-year quasi-cycles may also
363 correspond to the quasi-biennial oscillation (Labitzke and van Loon, 1999) and the tropospheric biennial oscillation
364 (Meehl, 1987). Despite the fact that many authors links 2-7-year cycles with El Niño–Southern Oscillation (ENSO) or
365 quasi-biennial oscillation in northeastern Asia, we didn't find significant correlation between the August–December
366 minimum temperature reconstruction and Nino3, but analysis showed significant correlation between the
367 reconstruction and temperature of Northern Hemisphere oceans. Probably, this means that the temperature variations
368 are more associated with the influence of PDO than ENSO.

369 On the decadal timescale analysis showed 20-year cycles which reflect processes influenced by Pacific Decadal
370 Oscillation (PDO, Mantua and Hare 2002) variability, which has been found at 15-25-yr and 50-70-yr cycles (Ma,
371 2007). Our analysis indicated a high significant correlation ($r=0.68$, $p<0.0001$) between reconstruction and the mean
372 annual PDO index of Mann *et al.* (2009) from 1900-2000. Taking into account that many researchers working in the
373 territory of northeast Asia have also revealed these cycles in relation to the Korean pine, we can draw a conclusion
374 that the Korean pine tree-ring series support the concept of long-term, multidecadal variations in the Pacific (e.g.,
375 D'Arrigo *et al.*, 2001; Cook, 2002; Jacoby *et al.*, 2004; Liu *et al.*, 2009; Li, Wang, 2013; Willes *et al.*, 2014; Lu, 2016)
376 and that such variation or shifts have been present in the Pacific for several centuries.

377 We suppose that 9-year cycle may correspond to solar activity because, firstly, many authors showed influence of
378 solar activity on the climate variability (Bond *et al.*, 2001; Lean *et al.*, 1999; Lean, 2000; Mann *et al.*, 2009; Zhu *et al.*
379 *et al.*, 2016). Secondly, the significant correlation between of the August–December minimum temperature
380 reconstruction and TSI can be regarded as an additional evidence of this assumption. And, finally, there is a
381 coincidence of the reconstructed cold periods with the Maunder Minimum (1645–1715) and the Dalton minimum
382 period centered in 1810.

383 Despite the fact that it is quite difficult to reveal for certain long-period cycles in a 486-year chronology, we
384 nonetheless revealed the 189-year cycle (MTM) or 200-year cycle (SSA analysis). Such periodicity is revealed in
385 long-term climate reconstructions and is linked to the quasi-200-year solar activity cycle in other study (Raspopov *et al.*
386 *et al.*, 2008; Raspopov *et al.*, 2009). In Raspopov *et al.* (2008) it was showed that the cycle varies in tree-ring based
387 reconstructions from 180 to 230 years. In addition, a high correlation between the minimum temperatures
388 reconstruction and TSI and also revealed link of the reconstructed temperatures and solar activity minima gives
389 grounds to propose that the driver of this 200-year cycle is the solar activity. Such climate cycling, linked not only to
390 temperature but also to precipitation, is revealed for the territories of Asia, North America, Australia, Arctic and
391 Antarctic (Raspopov *et al.*, 2008). At the same time, the 200-year cycle (*de-Vries* cycle) may often have a phase shift
392 from some years to decades and correlates not only positively but also negatively with climatic fluctuations depending
393 on the character of the nonlinear response of the atmosphere-ocean system within the scope of the region (Raspopov
394 *et al.*, 2009). According to Raspopov *et al.* (2009), the study area is in the zone that reacts with a positive correlation
395 to solar activity, though the authors note that we should not expect a direct response because of the nonlinear character
396 of the atmosphere-ocean system reaction to variability in solar activity (Raspopov *et al.*, 2009). Taking into
397 consideration this fact and that the cold and warm periods shown in our reconstruction are slightly shifted compared
398 with more continental areas and the whole Northern Hemisphere, we can say that the reconstruction of minimum
399 August–December temperatures reflects the global climate change process in aggregate with the regional
400 characteristics of the study area.

401 Conclusions

402 Using the tree-ring width of *Pinus koraiensis*, the mean minimum temperature of the previous August-December has
403 been reconstructed for the southern part of Sikhote-Alin Mountain Range, northeastern Asia, Russia, for the past 486
404 years. This dataset is the first climate reconstruction for this region, and for the first time for northeast Asia, we present
405 a reconstruction with a length exceeding 486 years.
406 Because explained variance of our reconstruction is about 39%, we believe that the result is noteworthy as it displays
407 the respective temperature fluctuations for the whole region, including northeast China, the Korean peninsula and the
408 Japanese archipelago. Our reconstruction is also in good agreement with the climatic reconstruction for the whole
409 Northern Hemisphere. The reconstruction shows good agreement with the cold periods described by documentary
410 notes in eastern China and Japan. All these comparisons prove that for this region, the climatic reconstruction based
411 on tree-ring chronology has a good potential to provide a proxy record for long-term, large-scale past temperature
412 patterns for northeast Asia. The results show the cold and warm periods in the region, which are conditional on global
413 climatic processes (PDO), and reflect the influence of solar activity (we revealed a correlation of the minimum
414 temperature variation and the 9-11-year and 200-year solar activity cycles). At the same time, the reconstruction
415 highlights the peculiarities of the flows of global process in the study area and helps in understanding the processes
416 in the southern territory of the Russian Far East for more than the past 450 years. Undoubtedly, the results of our
417 research are important for studying the climatic processes that have occurred in the study region and in all of
418 northeastern Asia and for situating them within the scope of global climatic change.

419

420 **Acknowledgements** This work was funded by Russian Foundation for Basic Research, Project 15-04-02185.

421 **References**

- 422 Anchukaitis K.J., D'Arrigo R.D., Andreu-Hayles L., Frank D., Verstege A., Curtis A., Buckley B.M., Jacoby G.C.,
423 and Cook E.R.: Tree-ring-reconstructed summer temperatures from Northwestern North America during the last
424 nine centuries. *J Clim.* 26, 3001-3012, doi: 10.1175/JCLI-D-11-00139.1, 2013.
- 425 Bard E., Raisbeck G., Yiou F. and Jouzel J.: Solar irradiance during the last 1200 years based on cosmogenic
426 nuclides. *Tellus B.*, 52, 985-992, 2000.
- 427 Bazarova V.B., Grebennikova T.A., and Orlova L.A.: Natural-environment dynamic within the Amur basin during
428 the neoglacal. *Geogr. Nat. Resour.*, 35(3), 275-283, doi: 10.1134/S1875372814030111, 2014.
- 429 Bond G., Kromer B., Beer J., Muscheler R., Evans M.N., Showers W., Hoffmann S., Lotti-Bond R., Hajdas I.,
430 Bonani G.: Persistent solar influence on north Atlantic climate during the Holocene. *Sci.*, 294, 2130–2136, 2001.
- 431 Borisova O.K.: Landscape-climatic changes in Holocene. *Reg. Res. Rus.*, 2, 5-20, 2014.
- 432 Bradley R.S., Diaz H.F., Kiladis G.N., Eischeid J.K.: ENSO signal in continental temperature and precipitation
433 records. *Nat.* 327, 497-501, 1987.
- 434 Dettinger M.D., Ghil M., Strong C.M., Weibel W., and Yiou, P.: Software expedites singular-spectrum analysis of
435 noisy time series, *Eos, Trans. American Geophysical Union* 76(2), 12, 14, 21, 1995.
- 436 Cook E.R., Kairiukstis L.A.: *Methods of dendrochronology: applications in the environmental sciences.* Kluwer
437 Academic Publishers, Dordrecht, 1990.
- 438 Cook E.R.: Reconstructions of Pacific decadal variability from long tree-ring records. *Eos Trans.* 83 (19) Spring
439 Meet. Suppl., Abstract GC42A-04, 2002.

440 Corona C., Guiot J., Edouard J.L., Chalié F., Büntgen U., Nola P. and Urbinati C.: Millennium-long summer
441 temperature variations in the European Alps as reconstructed from tree rings. *Clim. Past.*, 6, 379-400,
442 doi:10.5194/cp-6-379-2010, 2012.

443 Dai L.M., Qi L., Su D.K., Wang Q.W., Ye Y.J. and Wang Y.: Changes in forest structure and composition on
444 Changbai Mountain in Northeast China. *Ann. For. Sci.*, 68, 889-897, 2011.

445 Ding Y., Dai X.: Temperature Variation in China during the Last 100 years. *Meteorology*, 20, 19-26, 1994.

446 Durbin J. and Watson G.S.: Testing for serial correlation in least squares regression. *Biometrika*, 38, 159-178, 1951.

447 Efron B.: The jackknife, the bootstrap, and other resampling plans. Pa. Soc. for Industrial and Appl. Mathem.,
448 Philadelphia, 1982.

449 Efron B.: Bootstrap methods: another look at the jackknife. *Annals Statistics*, 7, 1-26, 1979.

450 Fritts H.C.: Tree rings and climate. Academic Press Inc., London, 1976.

451 Fukaiishi K. and Tagami Y.: An attempt of reconstructing the winter weather situations from 1720–1869 by the use
452 of historical documents. In: Proceedings of the International Symposium on the Little Ice Age Climate, Department
453 of Geography, Tokyo Metropolitan University, Tokyo, 194-201, 1992.

454 Ge Q., Zheng J., Hao Z., Liu Y. and Li M.: Recent advances on reconstruction of climate and extreme events in
455 China for the past 2000 years. *J Geogr Sci* 26(7), 827-854, doi: 10.1007/s11442-016-1301-4, 2016.

456 Ghil M., Allen R.M., Dettinger M.D., Ide K., Kondrashov D., Mann M.E., Robertson A., Saunders A., Tian Y.,
457 Varadi F. and Yiou P.: Advanced spectral methods for climatic time series. *Rev Geophys* 40(1), 3.1-3.41,
458 10.1029/2000RG000092, 2002.

459 Gou X., Chen F., Yang M., Gordon J., Fang K., Tian Q. and Zhang Y.: Asymmetric variability between maximum
460 and minimum temperatures in Northeastern Tibetan Plateau: evidence from tree rings. *Sci. China. Ser. D.* 51, 41-55,
461 2008.

462 Hirano J. and Mikami T.: Reconstruction of winter climate variations during the 19th century in Japan. *Int J*
463 *Climatol* 28, 1423-1434, doi:10.1002/joc.1632, 2007.

464 Holmes R.L.: Computer-assisted quality control in tree-ring dating and measurement. *Tree-ring Bull.* 43, 69-78,
465 1983.

466 Ishikawa Y., Krestov P.V. and Namikawa K.: Disturbance history and tree establishment in old-growth *Pinus*
467 *koraicensis*-hardwood forests in the Russian Far East. *J. Veg. Sci.* 10, 439-448, 1999.

468 Jacoby G., Solomina O., Frank D., Eremenko N. and D'Arrigo R.D.: Kunashir (Kuriles) Oak 400-year
469 reconstruction of the temperature and relation to the Pacific Decadal Oscillation. *Palaeogeogr Palaeoclimatol*
470 *Palaeoecol*, 2009, 303-311, doi: 10.1016/j.paleo.2004.02.015, 2004.

471 Karl T.R., Jones P.D., Knight R.W., Kulas G., Plummer N., Razuvayev V., Gallo K.P., Lindsey J., Charlson R.J.,
472 and Peterson T.C.: A new perspective on recent global warming: asymmetric trends of daily maximum and
473 minimum temperature. *B. Am. Meteorol. Soc.*, 74, 1007-1023, 1993.

474 Kolesnikov B.P.: Korean pine forests of the [Russian] Far East. *Trudy DVF AN SSSR.* 2, 1-264, 1956 (In Russian).

475 Körner C. and Paulsen J.: A world-wide study of high altitude treeline temperatures. *J. Biogeogr.*, 31, 713-732,
476 doi:10.1111/j.1365-2699.2003.01043.x, 2004.

477 Kozhevnikova N.K.: Dynamics of weather-climatic characteristics and ecological function of small river basin. *Sib.*
478 *Ecol. J.*, 5, 93-703, 2009 (In Russian).

479 Kress A., Hangartner S., Bugmann H., Büntgen U., Frank D.C., Leuenberger M., Siegwolf R.T.W. and Saurer M.:
480 Swiss tree rings reveal warm and wet summers during medieval times. *Geophys. Res. Lett.*, 41, 1732-1737, doi:
481 10.1002/2013GL059081, 2014.

482 Labitzke K.G. and van Loon H.: The Stratosphere: Phenomena, History and Relevance. Springer, Berlin, 1999.

483 Lean J.: Evolution of the Sun's spectral irradiance since the Maunder Minimum. *Geophys. Res. L.*, 27(16), 2425-

484 2428, doi: 10.1029/2000GL000043, 2000.

485 Lean J. and Rind D.: Evaluating sun-climate relationships since the Little Ice Age. *J. Atmos. Sol. Terr. Phys.*, 61,

486 25-36, 1999.

487 Li M. and Wang X.: Climate-growth relationships of three hard- wood species and Korean pine and minimum

488 temperature reconstruction in growing season in Dunhua, China. *J. Nanjing. For. Univ.*, 37, 29-34, 2013.

489 Liu Y., Bao G., Song H., Cai Q. and Sun J.: Precipitation reconstruction from Hailar pine (*Pinus koraiensis* var.

490 *mongolica*) tree rings in the Hailar region, Inner Mongolia, China back to 1865 AD. *Paleogeogr Paleoclimatol*

491 *Paleoecol*, 282, 81-87, doi:10.1016/j.palaeo.2009.08.012, 2009.

492 Liu Q.J.: Structure and dynamics of the subalpine coniferous forest on Changbai mountain, China. *Plant. Ecol.* 132,

493 97-105, 1997.

494 Lu R., Jia F., Gao S., Shang Y. and Chen Y.: Tree-ring reconstruction of January-March minimum temperatures

495 since 1804 on Hasi Mountain, northwestern China. *J. Arid. Environ.*, 127, 66-73,

496 doi:10.1016/j.jaridenv.2015.10.020, 2016.

497 Lyu S., Li Z., Zhang Y. and Wang X.: A 414-year tree-ring-based April–July minimum temperature reconstruction

498 and its implications for the extreme climate events, northeast China. *Clim. Past.* 12, 1879-1888, doi:10.5194/cp-12-

499 1879-2016, 2016.

500 Ma Z.G.: The interdecadal trend and shift of dry/wet over the central part of north China and their relationship to the

501 Pacific Decadal Oscillation (PDO). *Chin. Sci. Bull.*, 52(12), 2130-2139, 2007.

502 Mann M.E. and Lees J.M.: Robust estimation of background noise and signal detection in climatic time series. *Clim.*

503 *Change*, 33, 409-445, 1996.

504 Mann M.E., Zhang Z., Rutherford S., Bradley R.S., Hughes M., Shindell D., Amman C., Faluvegi G. and Ni F.:

505 Global Signatures and Dinamical Origins of the Little Ice Age and Medieval Climate Anomaly. *Science*, 326, 1256-

506 1260, doi:10.1126/science.1177303, 2009.

507 Mantua N., Hare S.: The Pacific decadal oscillation. *J. Oceanogr.* 58(1), 35-44, 2002.

508 Meehl G.A.: The annual cycle and interannual variability in the tropical Pacific and Indian Ocean regions. *Mon.*

509 *Weather. Rev.*, 115, 27-50, 1987.

510 Melvin T.M. and Briffa K.R.: A 'signal-free' approach to dendroclimatic standardisation. *Dendrochronologia*, 26,

511 71-86, doi: 10.1016/j.dendro.2007.12.001, 2008.

512 Nishimura M. and Yoshikawa I.: Nippon Kyokoshi Ko, Maruzen, Tokyo, an archival collection of disasters in

513 Japan, 1936 (in Japanese)

514 Ohayama M., Yonenobu H., Choi J.N., Park W.K., Hanzawa M. and Suzuki M.: Reconstruction of northeast Asia

515 spring temperature 1784-1990. *Clim. Past.*, 9, 261-266, doi:10.5194/cp-9-261-2013, 2013.

516 Omelko A., Ukhvatkina O. and Zmerenetsky A.: Disturbance history and natural regeneration of an old-growth

517 Korean pine-broadleaved forest in the Sikhote-Alin mountain range, Southeastern Russia. *For. Ecol. Manag.* 360,

518 221-234, doi: 10.1016/j.foreco.2015.10.036, 2016.

519 Omelko A.M. and Ukhvatkina, O.N.: Characteristics of gap-dynamics of conifer-broadleaved forest of Southen

520 Sikhote-Alin (Russia). *Plant World Asian Russ.*, 1, 106-113, 2012.

521 Popa I. and Bouriaud O.: Reconstruction of summer temperatures in Eastern Carpathian Mountain (Rodna Mts,

522 Romania) back to AD 1460 from tree-rings. *Int. J. Climatol.*, 34, 871-880, doi: 10.1002/joc.3730, 2014.

523 Porter T.J., Pisaric M.F., Kokelj S.V. and DeMontigny P.: A ring-width-based reconstruction of June-July minimum
524 temperatures since AD 1245 from white spruce stands in the Mackenzie Delta region, northwestern Canada.
525 Quaternary. Res., 80, 167-179, doi: 10.1016/j.yqres.2013.05.004, 2013.

526 Raspopov OM, Dergachev VA, Esper J, Kozyreva OV, Frank D, Ogurtsov M, Kolström T, Shao X (2008) The
527 influence of the de Vries (~200-year) solar cycle on climate variations: Results from the Central Asian
528 Mountains and their global link. *Palaeogeogr Palaeoclimatol Palaeoecol*, 259, 6-16. doi:
529 10.1016/j.palaeo.2006.12.017

530 Raspopov O.M., Dergachev V.A., Kozyreva O.V., Kolström T., Lopatin E.V. and Luckman B.: Geography of 200-
531 year climate periodicity and Long-Term Variations of Solar activity. *Reg. Res. Russ.*, 2, 17-27, 2009.

532 Razzhigaeva N.G., Ganzei L.A., Mokhova L.M., Makarova T.R., Panichev A.M., Kudryavtseva E.P., Arslanov
533 Kh.A., Maksimov F.E. and Starikova A.A.: The Development of Landscapes of the Shkotovo Plateau of Sikhote-
534 Alin in the Late Holocene. *Reg. Res. Russ.*, 3, 65-80, doi:10.15356/0373-2444-2016-3-65-80, 2016.

535 Ren F. and Zhai P.: Study on Changes of China's Extreme Temperatures During 1951–1990. *Sci. Atmos. Sin.*, 22,
536 217-227, 1998.

537 Sakaguchi Y.: Warm and cold stages in the past 7600 years in Japan and their global correlation. *Bull. Dep. Geogr.*
538 15, 1-31, 1983.

539 Shao X. and Wu X.: Reconstruction of climate change on Changbai Mountain, Northeast China using tree-ring data.
540 *Quaternary. Sci.*, 1, 76-83, 1997.

541 Stokes M.A. and Smiley T.L.: *Tree-ring dating*. The University of Chicago Press, Chicago, London, 1968.

542 Tang H., Zhai P. and Wang Z.: On Change in Mean Maximum Temperature, Minimum Temperature and Diurnal
543 Range in China During 1951–2002. *Climatic Environ Res.*, 10, 728-735, 2005.

544 Thapa U.K., Shan S.K., Gaire N.P. and Bhujju D.R.: Spring temperatures in the far-western Nepal Himalaya since
545 1640 reconstructed from *Picea smithiana* tree-ring widths. *Clim dyn*, 45(7), 2069-2081, doi: 10.1007/s00382-014-
546 2457-1, 2015.

547 Wang H., Shao X.M., Jiang Y., Fang X.Q. and Wu S.W.: The impacts of climate change on the radial growth of
548 *Pinus koraiensis* along elevations of Changbai Mountain in northeastern China. *For. Ecol. Manag.*, 289, 333-340,
549 doi:10.1016/j.foreco.2012.10.023, 2013.

550 Wang X., Zhang M., Ji Y., Li Z., Li M. and Zhang Y.: Temperature signals in tree-ring width and divergent
551 growth of Korean pine response to recent climate warming in northeast Asia. *Trees* 31(2), 415-427, doi:
552 10.1007/s00468-015-1341-x, 2016.

553 Wang S., Liu J. and Zhou J.: The Climate of Little Ice Age Maximum in China. *J. Lake. Sci.*, 15, 369-379, 2003.

554 Wang W., Zhang J., Dai G., Wang X., Han S., Zhang H. and Wang Y.: Variation of autumn temperature over the
555 past 240 years in Changbai Mountain of Northeast China: A reconstruction with tree-ring records. *China. J. Ecol.*,
556 31, 787-793, 2012.

557 Wang Z., Ding Y., He J. and Yu J.: An updating analysis of the climate change in China in recent 50 years. *Ac*
558 *Meteorol Sin*, 62, 228-236, 2004.

559 Wigley T.M.L., Briffa K.R. and Jones P.D.: On the average value of correlated time series, with applications in
560 dendroclimatology and hydrometeorology. *J. Clim. Appl. Meteorol.*, 23, 201-213, 1984.

561 Wiles G.C., Solomina O., D'Arrigo R., Anchukaitis K.J., Gensiarovsky Y.V. and Wiesenberg N.: Reconstructed
562 summer temperatures over the last 400 year a based on larch ring widths: Sakhalin Island, Russian Far East. *Clim.*
563 *Dyn.*, 45, 397-405, doi: 10.1007/s00382-014-2209-2, 2014.

564 Wilson R.J.S. and Luckman B.H.: Tree-ring reconstruction of maximum and minimum temperatures and the diurnal
565 temperature range in British Columbia, Canada. *Dendrochronologia*, 20, 1-12, 2002.

566 Wilson R.J.S., Luckman B.H.: Dendroclimatic reconstruction of maximum summer temperatures from upper
567 treeline sites in Interior British Columbia, Canada. *Holocene*, 13, 851-861, doi:10.1191/0959683603hl663rp, 2003.

568 Xie Z. and Cao H.: Asymmetric changes in maximum and minimum temperature in Beijing. *Theor Appl Climatol*,
569 55, 151-56, 1996.

570 Yin H., Guo P., Liu H., Huang L., Yu H., Guo S. and Wang F.: Reconstruction of the October mean temperature
571 since 1796 at Wuying from tree ring data. *Adv. Clim. Change. Res.*, 5, 18-23, 2009.

572 Yin H., Liu H., Linderholm H.W. and Sun Y.: Tree ring density-based warm-season temperature reconstruction
573 since AD 1610 in the eastern Tibetan Plateau. *Palaeogeogr, Palaeoclimatol, Palaeoecol*, 426, 112-120, doi:
574 10.1016/j.palaeo.2015.03.003, 2015.

575 Young G.A.: Bootstrap: more than a stab in the dark. *Statistical. Sci.* 9, 382-415, 1994.

576 Zaiki M., Können G., Tsukahara T., Jones P., Mikami T. and Matsumoto K.: Recovery of nineteenth-century
577 Tokyo/Osaka meteorological data in Japan. *Int J Climatol*, 26, 399-423, doi:10.1002/joc.1253, 2006.

578 Zang C. and Biondi F.: Treeclim: an R package for the numerical calibration of proxy-climate relationships. *Ecogr.*
579 38, 001-006, doi: 10.1111/ecog.01335, 2015.

580 Zhang R.B., Yuan Y.J., Wei W.S., Gou X.H., Yu S.L., Shang H.M., Chen F., Zhang T.W. and Qin L.:
581 Dendroclimatic reconstruction of autumn-winter mean minimum temperature in the eastern Tibetan Plateau since
582 1600 AD. *Dendrochronologia*, 33, 1-7, doi: 10.1016/j.dendro.2014.09.001, 2015.

583 Zhao C., Ring G., Zhang Y., Wang Y.: Climate change of the Northeast China over the past 50 years. *J. Arid. Land.*
584 *Resour. Environ.*, 23, 25-30, 2009.

585 Zhu H.F., Fang X.Q., Shao X.M. and Yin Z.: Tree-ring-based February-April temperature reconstruction for
586 Changbai Mountain in Northeast China and its implication for East Asia winter monsoon. *Clim Past.*, 5, 661-666,
587 2009.

588 Zhu L., Li Z., Zhang Y. and Wang X.: A 211-year growing season temperature reconstruction using tree-ring width
589 in Zhangguangcai Mountains, Northeast China: linkages to the Pacific and Atlantic Oceans. *Int. J. Climatol.*, doi:
590 10.1002/joc.4906, 2016.

591 Zhu L., Li S., Wang X.: Tree-ring reconstruction of February-March mean minimum temperature back to 1790 AD
592 in Yichun, Northeast China. *Quaternary. Sci.*, 35, 1175-1184, doi: 10.11928/j.issn.1001-7410.2015.05.13, 2015.

593 **Tables and Figures**

594 **Table 1.** The sampling information and statistics of the signal-free chronology

	VUSr
Elevation (m a.s.l.)	700-900
Latitude (N), Longitude (E)	44°01'32'', E 134°13'15''
Core (live trees) / sample (dead trees)	25/20
Time period / length (year)	1451-2014 / 563
MS	0.253
SD	0.387
AC1	0.601
R	0.691
EPS	0.952
Period with EPS>0.85 / length (year)	1602-2014 / 412
Period with EPS>0.75 / length (year)	1529-2014 / 485
Skew/Kurtosis	0.982/5.204

595 MS – mean sensitivity, SD – standard deviation, AC1 – first-order autocorrelation, EPS – expressed population signal

596

597 **Table 2.** Calibration and verification statistics of the reconstruction equation for the common period 1971-2003 of

598 **Bootstrap**

Statistical item	Calibration	Verification (Bootstrap, 199 iterations)
r	0.62	0.62 (0.54-0.70)
R ²	0.39	0.39 (0.37-0.41)
R ² _{adj}	0.36	0.37 (0.37-0.40)
Standard error of estimate	1.20	1.11
F	18.76	18.54
P	0.0001	0.0001
Durbin-Watson	1.73	1.80

599

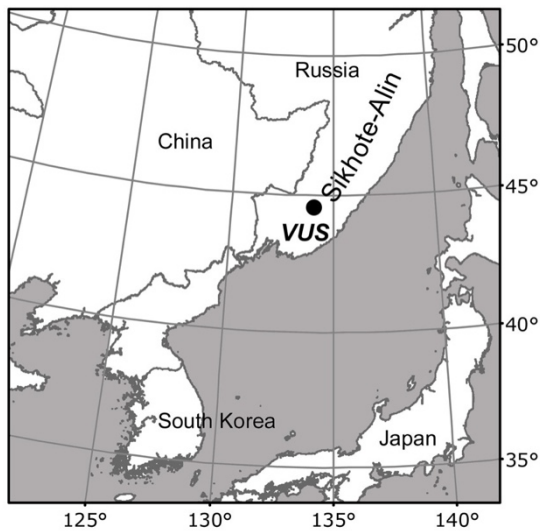
600 **Table 3.** Cold and warm periods based on the results of this study compared with other researches

Period	Southern Sikhote-Alin (this study)	Laobai Mountain (Lyu et al., 2016)	Changbai Mountain (Zhu et al., 2009)
Cold	1538-1544; 1549-1554	*	*
	—	1605-1616	
	1643-1649; 1659-1667	1645-1677	*
	1675-1689	1684-1691	*
	1791-1801; 1807-1818	—	1784-1815
	1822-1827; 1836-1852		1827-1851
	1868-1887	—	1878-1889
	1911-1925	1911-1924; 1930-1942; 1951-1969	1911-1945
Warm	1561-1584	*	*

1603-1607; 1614-1618	—	*
1738-1743	—	—
1756-1759; 1776-1781	1767-1785	1750-1783
<i>1787-1793**</i>	1787-1793	—
<i>1795-1807**</i>	1795-1807	—
<i>1855-1865**</i>	—	1855-1877
1944-2014	1991-2008	1969-2009

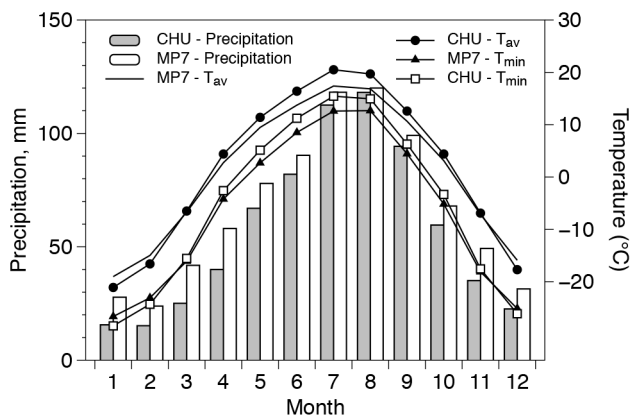
601 Note: *italic *** – the periods which agreement with VUSr but not reliably for VUSr; * - the reconstruction not
602 covering this period.

603



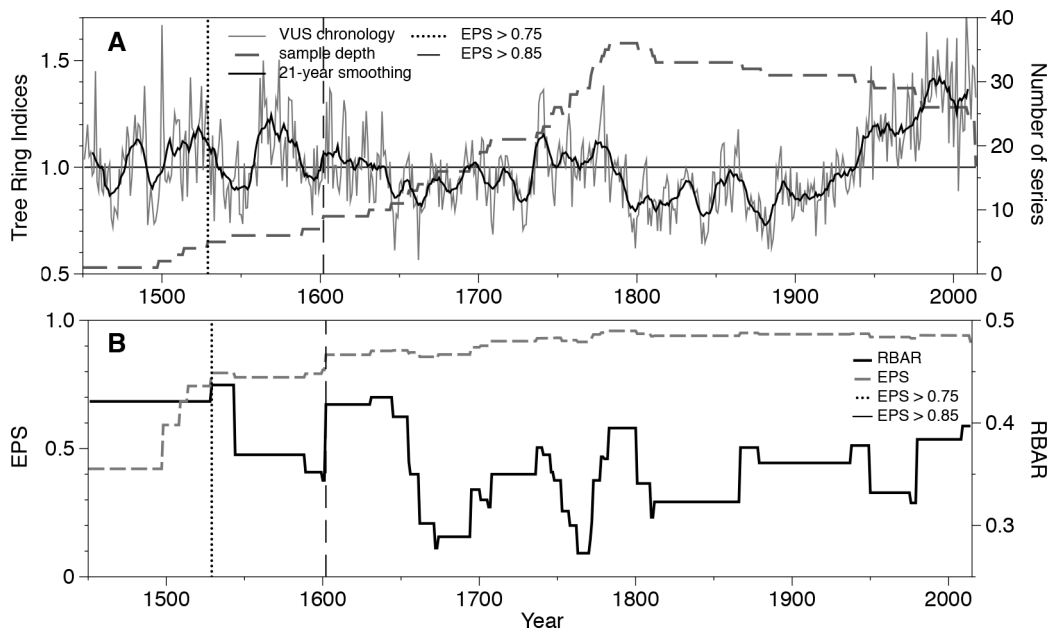
604

605 **Figure 1:** Location of the study area on the Sikhote-Alin Mountains, Southeastern Russia. VUS is Verkhneussyriysky
606 Research Station



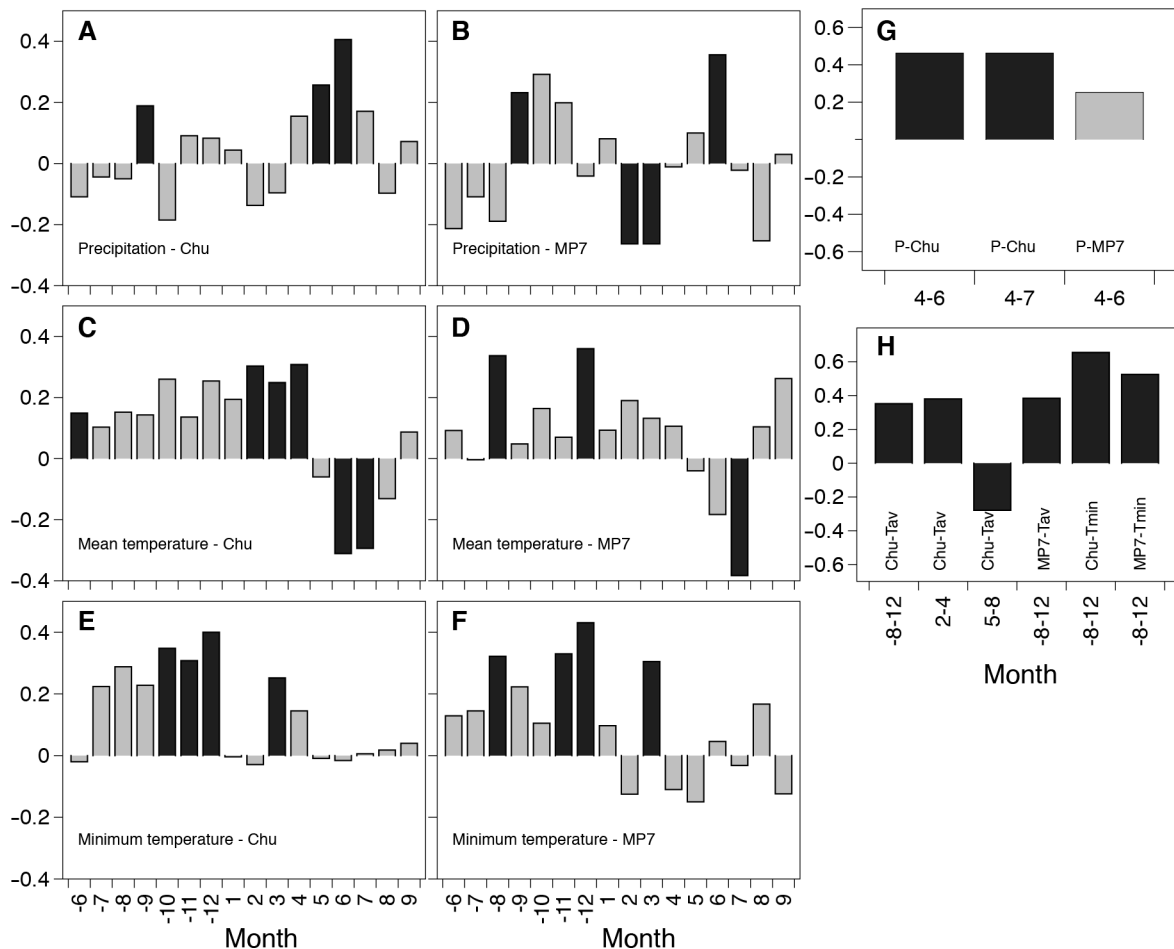
607

608 **Figure 2:** Mean monthly (1936-2004), minimum temperature (1971-2003) and total precipitation (1936-2004) at
609 Chuguevka and mean monthly, minimum temperature and total precipitation for VUS meteorological station (MP7)
610 (1966-2000)



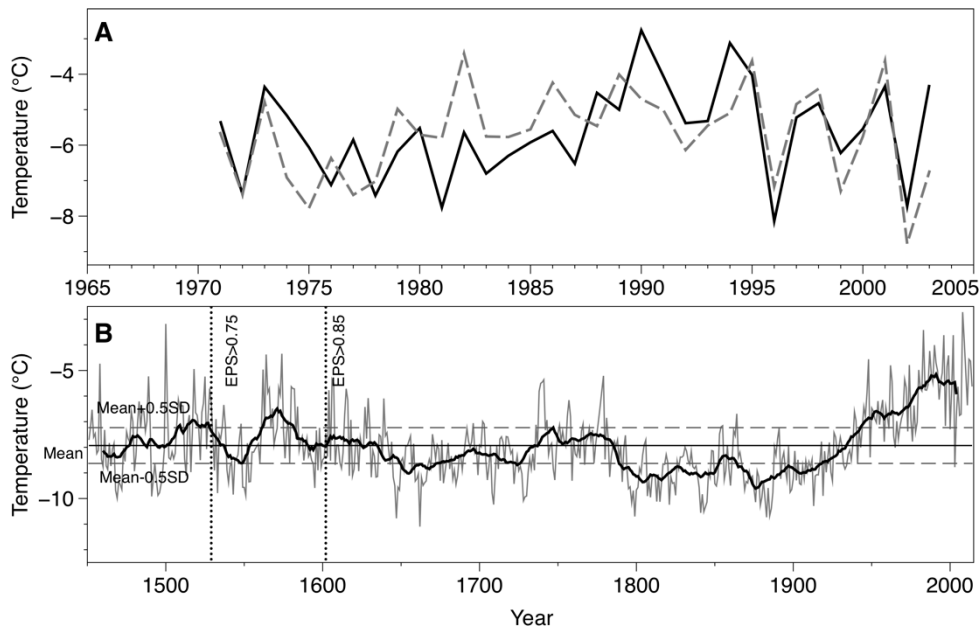
611
612
613

Figure 3: Variations of the VUS chronology and sample depth (a) and the expressed population signal (EPS) and average correlation between all series (Rbar) VUS chronology from AD 1451 to 2014 (b)



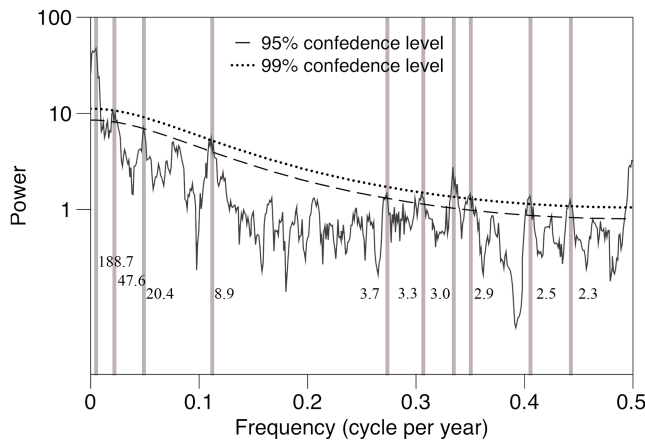
614
615
616
617
618
619

Figure 4: Correlations between the monthly mean meteorological data and VUS chronology
A, C, E – Chuguevka (Chu) and VUS chronology; B, D, F - VUS meteorological station (MP7) and VUS chronology;
G – correlation coefficients between VUS chronology and the precipitation of different month combinations; H –
correlation coefficients between VUS chronology and the temperature of different month combinations. The black
bars are significant value.



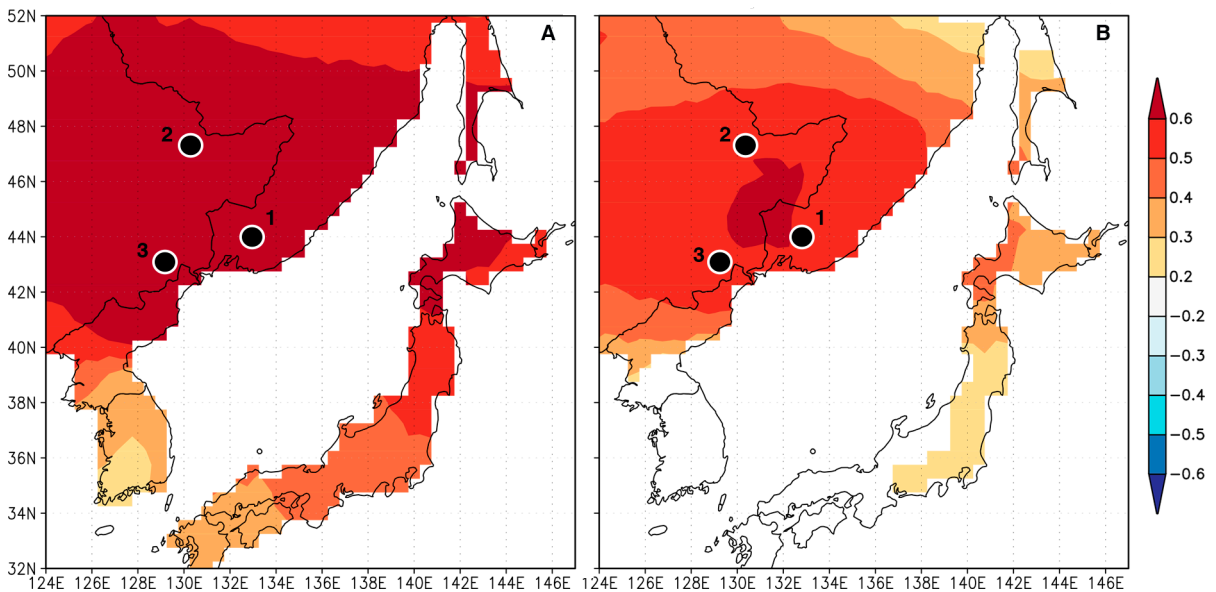
620
621
622
623

Figure 5: (a) Actual (black line) and reconstructed (dash line) August – December minimum temperature for the common period of 1971-2003; (b) reconstruction of August – December minimum temperature (VUSr) to Southern part of Sikhote-Alin for the last 563 years. The smoothed line indicates the 21-year moving average.



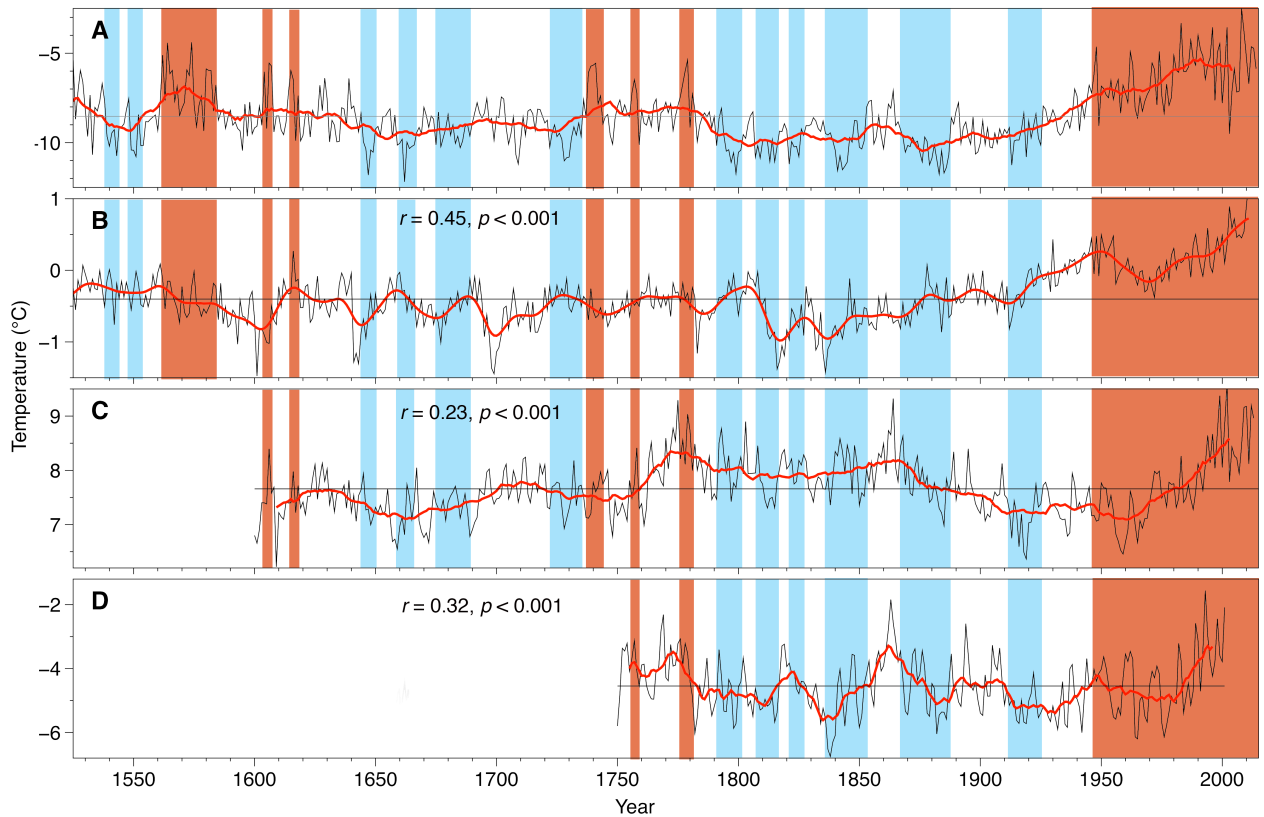
624
625
626

Figure 6: The MTM power spectrum of the reconstructed August – December minimum temperature (VUSr) from 1529 to 2014



627

628 **Figure 7:** Spatial correlations between the observed (a) and reconstructed (b) August – December minimum
 629 temperature (VUS) in this study and regional gridded annual minimum temperature from CRU TS 4.00 over their
 630 common period 1960–2003 ($p < 10\%$). Location of compared temperature reconstructions: (1) August-December
 631 mean minimum temperature reconstructed (VUSr) on southern part of Sikhote-Alin, (2) April – July minimum
 632 temperature on Laobai Mountain by Lyu et al., 2016, and (3) February – April temperature established by Zhu et al.
 633 (2009) on Changbai Mountain.
 634



635
 636 **Figure 8:** (a) August-December mean minimum temperature reconstructed (VUSr) on southern part of Sikhote-
 637 Alin, (b) Northern Hemisphere extratropical temperature (Willes et al., 2016), (c) April – July minimum temperature
 638 on Laobai Mountain by Lyu et al., 2016, and (d) February – April temperature established by Zhu et al. (2009) on
 639 Changbai Mountain. Black lines denote temperature reconstruction values, and red color lines indicate the 21-year
 640 moving average; red and blue fields – warm and cold period consequently (in this study)